

Original Article

# Targeting GRP78 enhances the sensitivity of HOS osteosarcoma cells to pyropheophorbide- $\alpha$ methyl ester-mediated photodynamic therapy via the Wnt/ $\beta$ -catenin signaling pathway

Qiang Zuo<sup>†</sup>, Yunsheng Ou<sup>\*</sup>, Shenxi Zhong<sup>†</sup>, Haoyang Yu<sup>†</sup>, Fangbiao Zhan, and Muzi Zhang

Department of Orthopedics, The First Affiliated Hospital of Chongqing Medical University, Chongqing 400016, China

<sup>†</sup>These authors contributed equally to this work.

\*Correspondence address. Tel: +86-18696669666; E-mail: [ouyunsheng2001@163.com](mailto:ouyunsheng2001@163.com)

Received 4 March 2021; Editorial Decision 31 May 2021

## Abstract

Photodynamic therapy (PDT), which is a new method for treating tumors, has been used in the treatment of cancer. In-depth research has shown that PDT cannot completely kill tumor cells, indicating that tumor cells are resistant to PDT. Glucose regulatory protein 78 (GRP78), which is a key regulator of endoplasmic reticulum stress, has been confirmed to be related to tumor resistance and recurrence, but there are relatively few studies on the further mechanism of GRP78 in PDT. Our experiment aimed to observe the role of GRP78 in HOS human osteosarcoma cells treated with pyropheophorbide- $\alpha$  methyl ester-mediated photodynamic therapy (MPP $\alpha$ -PDT) and to explore the possible mechanism by which the silencing of GRP78 expression enhances the sensitivity of HOS osteosarcoma cells to MPP $\alpha$ -PDT. HOS osteosarcoma cells were transfected with siRNA-GRP78. Apoptosis and reactive oxygen species (ROS) levels were detected by Hoechst staining and flow cytometry, cell viability was detected by Cell Counting Kit-8 assay, GRP78 protein fluorescence intensity was detected by immunofluorescence, and apoptosis-related proteins, cell proliferation-related proteins, and Wnt pathway-related proteins were detected by western blot. The results showed that MPP $\alpha$ -PDT can induce HOS cell apoptosis and increase GRP78 expression. After successful siRNA-GRP78 transfection, HOS cell proliferation was decreased, and apoptosis-related proteins expressions was increased, Wnt/ $\beta$ -catenin-related proteins expressions was decreased, and ROS levels was increased. In summary, siRNA-GRP78 enhances the sensitivity of HOS cells to MPP $\alpha$ -PDT, the mechanism may be related to inhibiting Wnt pathway activation and increasing ROS levels.

**Key words:** glucose regulated protein 78, osteosarcoma, photodynamic therapy, pyropheophorbide- $\alpha$  methyl ester, Wnt signaling pathway, reactive oxygen species

## Introduction

Osteosarcoma is a common primary malignant tumor of the bone that occurs in adolescent patients. It usually occurs in the distal femur and proximal tibia [1]. With advances in medical technology and the emergence of neoadjuvant treatments, the overall survival rate of patients has improved, but osteosarcoma recurs, and transfer is still

a difficult problem for treatment [2]. Photodynamic therapy (PDT) is a new method for treating malignant tumors with a short treatment time window, few side effects and is conducive to repeated treatment. The main mechanism of PDT is the production of a large amount of reactive oxygen species (ROS) and the initiation of tumor cell apoptosis, it has been used in skin tumor treatment [3–6].

Glucose regulatory protein 78 (GRP78) is a member of the heat shock protein 70 family and a key regulatory protein of endoplasmic reticulum (ER) stress, regulates the unfolded protein response by maintaining the calcium homeostasis of the ER and controlling the activation of sensors so that the cellular microenvironment can be restored to a steady state [7–9]. It is highly expressed in various malignant tumors [10–12]. In addition to its strong antiapoptotic properties, GRP78 is also closely related to tumor proliferation and survival. Studies have shown that GRP78 is one of the key regulators of tumor resistance and is closely related to tumor recurrence and metastasis [13,14]. The Wnt signaling pathway is a group of signal transduction pathways that includes multiple downstream channels that are stimulated by the binding of ligand proteins to membrane protein receptors. Through the activation of the intracellular segments of cell surface receptors, extracellular signals are transmitted into cells to play biological roles [15,16]. Studies have shown that the Wnt signaling pathway is a classic drug resistance pathway that plays a key role in tumor cell proliferation [17].

Silencing GRP78 has been reported to enhance the effects of tumor radiotherapy and chemotherapy. Although it has been proved that PDT can induce ER stress and increase the expression of GRP78, there are relatively few studies on the further mechanism of GRP78 in PDT [18–22]. This study will use siRNA-GRP78 to interfere with the expression of GRP78 in human HOS cells and explore the effects of MPP $\alpha$ -PDT on the proliferation activity, apoptosis level, ROS level, and Wnt signaling pathway activation of HOS cells.

## Materials and Methods

### Cell and cell culture

The human osteosarcoma HOS cell line was purchased from the Chinese Academy of Sciences (Shanghai, China), and cultured in DMEM (HyClone, Logan, USA), which contained 0.1 mg/ml streptomycin, 100 U/ml penicillin, and 10% fetal bovine serum. The cells were placed in an incubator at 37°C in 5% CO<sub>2</sub> and protected from light. When the cell density reached 60%–70%, routine passaging was performed.

### PDT treatment on HOS cells

Human osteosarcoma HOS cells in the logarithmic phase of growth were subjected to routine trypsin digestion and passaged into groups based on the experiment. When the cell growth density was approximately 50%–60%, the photosensitizer MPP $\alpha$  (Sigma-Aldrich, St Louis, USA) was added at a final concentration of 0.15  $\mu$ M, and the cells were incubated for 20 h in the dark. Continuous output mode was used with wavelengths of 630 nm and 40 mW/cm<sup>2</sup>, followed by 120 s of light, incubation in the dark in an incubator with a volume fraction of 5% CO<sub>2</sub> at 37°C, and incubation in accordance with the experimental groups [23].

### Hoechst staining and flow cytometry

Human osteosarcoma HOS cells in the logarithmic phase of growth were collected. After treatment, Hoechst fixative was added to each well for 15 min of fixation according to the manufacturer's (Beyotime Biotechnology Co., Ltd, Shanghai, China) instructions, and the cells were washed with PBS. Then, 1 ml of Hoechst 33258 dye was added to each well for 5 min, the residual dye was washed with PBS, and the changes in the cell nuclei in each group were observed by inverted fluorescence microscopy (Nikon, Tyoko, Japan).

After processing the cells according to experimental groups, the cells were washed three times with PBS buffer, trypsinized, and

centrifuged. Then, the supernatant was discarded, and the cell pellets from each group were collected. Three groups of cell samples were double stained with Annexin V-PI reagent (Beyotime Biotechnology Co., Ltd), and the apoptosis rate was detected by flow cytometry (BD Bioscience, Franklin Lakes, USA).

### siRNA transfection

HOS cells in the logarithmic phase of growth were seeded in a 6-well plate, and the cells were grouped as follows: Control group, siRNA negative control (siRNA-NC) group, and siRNA-GRP78 group. The siRNA targeting the GRP78 gene (siRNA-GRP78) was synthesized by Hanbio Biotechnology Co., Ltd (Shanghai, China), and the sequence was as follows: (siRNA-GRP78#1: sense: 5'-CCAAAGACGCGGAACUAUTT-3', antisense: 5'-AUAGUCCAGCGUCUUUGGTT-3'), (siRNA-GRP78#2: sense: 5'-GCUCGACUCGAAUCCAAATT-3', antisense: 5'-UUUGGAAUUCGAGUCGAGCTT-3'). The sequence of the siRNA-NC was as follows: (sense: 5'-UUCUCCGAACGU GUCACGUdTdT-3', antisense: 5'-ACGUGACACGUUCGGA GAAdTdT-3'). In a 15 ml centrifuge tube, 125  $\mu$ l of DMEM was added to the HOS cells, and 100 pmol siRNA was added and mixed well. Then, 4  $\mu$ l of Lipo8000™ transfection reagent (Beyotime Biotechnology Co., Ltd) was added and incubated at room temperature for 20 min, and finally, 125  $\mu$ l of the above mixture was added to each well. The plates were gently shaken, and after transfection for 6 h, the medium was changed to complete medium. The cells were used for the next experiment after 72 h.

### Quantitative real-time PCR

After the cells were transfected with siRNA-GRP78, the RNA was extracted with the RNAiso (TaKaRa, Dalian, China). cDNA was reverse transcribed, and the samples were loaded sequentially using a 10  $\mu$ l loading system and analyzed using the following computer program: 1 cycle of 95°C for 30 s, 40 cycles of 90°C for 5 s, 60°C for 30 s, and 65°C for 5 s.  $\beta$ -actin was used as the internal reference, and the primer sequences were as follows:  $\beta$ -Actin (F) 5'-CTCCATCCTGGCCTCGCTGT-3', (R) 5'-GCTGTACCTTCACCGTTC-3'; GRP78 (F) 5'-CACGCCGTCCTATGTTCG-3', (R) 5'-AAATGTCTTTGTTCCACC-3'. The 2<sup>- $\Delta\Delta$ C<sub>q</sub></sup> method was used for standardization, and the relative expression of GRP78 mRNA was calculated [24].

### CCK-8 assay

Cells in the logarithmic phase of growth were seeded in a 96-well plate at 5000 cells/well. After division into the siRNA-NC group, siRNA-GRP78 group, siRNA-GRP78 + MPP $\alpha$ -PDT group, and MPP $\alpha$ -PDT group, the proliferation activity of the HOS cells was detected at 3, 6, 12, and 24 h after treatment. According to the operating instructions of the Cell Counting Kit-8 (CCK-8) detection kit (MedChemExpress Company, Shanghai, China), 10  $\mu$ l CCK-8 solution and 90  $\mu$ l DMEM mixture were added to each well and incubated for 1 h. The *D* value of each well was measured with a microplate reader at a wavelength of 450 nm. Five replicate wells were established in each group, the experiment was repeated three times, and the average value was taken to calculate the survival rate of the cells in each group. Cell survival rate (%) = (average *D* value of experimental group – *D* value of zero adjustment hole) / (average *D* value of blank group – *D* value of zero adjustment hole)  $\times$  100% [25].

### Immunofluorescence assay

HOS cells in the logarithmic phase of growth were seeded in a 6-well plate with 25 mm cell slides. After processing the cells according to experimental groups, the cells were fixed with 4% paraformaldehyde for 30 min, washed with PBS three times, lysed with 0.1% Triton X-100 (Beyotime Biotechnology Co., Ltd) for 15 min, blocked with goat anti-rabbit serum for 40 min, and incubated with rabbit polyclonal GRP78 antibody (ProteinTech Group, Inc. Wuhan, China) (diluted 1:100) overnight at 4°C. Cy3-labeled goat anti-rabbit IgG fluorescent secondary antibody (Bioss Biotechnology Co., Ltd, Beijing, China) was added to the cells in the dark and incubated for 40 min at room temperature. The cells were washed three times with PBS, the nuclei were stained with DAPI for 5 min, and the cells were washed with PBS to remove the residual DAPI. Then, the slides were mounted and observed with a fluorescence microscope (Nikon). Fluorescence intensity analysis was performed with ImageJ 1.52e.

### Detection of ROS by flow cytometry and fluorescence microscopy

HOS cells in the logarithmic phase of growth were treated according to the experimental group. The cells were washed three times with PBS, digested, and centrifuged. According to the method for the ROS Assay Kit (Beyotime Biotechnology Co., Ltd), the DCFH-DA probe was diluted with DMEM at a ratio of 100:900, and 1 ml of the mixture was added according to each group. The groups were mixed well, incubated with 5% CO<sub>2</sub> at 37°C for 30 min, centrifuged three times, and washed to remove the residual DCFH-DA probe. Flow cytometry was used to detect the ROS fluorescence intensity.

HOS cells in the logarithmic phase of growth were seeded in 6-well plates according to the experiment and washed three times with PBS after treatment. Then, 1 ml of the DCFH-DA probe dilution solution was added to each well according to the above ratio, and the cells were incubated in 5% CO<sub>2</sub> and 37°C for 30 min. Then, the cells were washed with PBS to remove the residual DCFH-DA probe, and the changes in ROS fluorescence intensity were observed with an inverted microscope.

### Western blot analysis

After processing the cells according to the experimental groups and extracting the cellular proteins, BCA kit was used to detect the protein concentration, and western blot was used to detect the expression of the relevant proteins. Briefly, HOS cells were lysed using cold RIPA buffer (Beyotime Biotechnology Co., Ltd) mixed with a phosphatase and protease inhibitor cocktail (Beyotime Biotechnology Co., Ltd). Following separation process via 10% or 12% SDS-PAGE, proteins were transferred to PVDF membranes (Beyotime Biotechnology Co., Ltd), which were sealed with 5% fat free milk for 2 h. The membranes were incubated with the following primary antibodies for more than 12 h at 4°C. GRP78 and p- $\beta$ -catenin antibodies were both from ProteinTech Group, Inc.;  $\beta$ -actin, cleaved caspase-3, and cleaved PARP antibodies were all purchased from Cell Signaling Technology, Inc. (Danvers, USA); Ki67, PCNA, AKT, GSK3 $\beta$ , and  $\beta$ -catenin antibodies were all from Servicebio Biotechnology Co., Ltd (Wuhan, China); and p-GSK3 $\beta$  and p-AKT antibodies were all from Boster Biological Technology Co., Ltd (Wuhan, China). Then, the rabbit HRP-conjugated monoclonal anti-IgG secondary antibody (Boster Biological Technology Co., Ltd) (1:8000) were added. The revelation was developed with a BiossECL Plus WB Substrate (Bioss, Beijing, China). Image Lab was used to analyze the target bands, and

the ratio of the gray value of the target protein to that of  $\beta$ -actin was used to express the relative expression of the target protein.

### Statistical analysis

The experimental data results were analyzed by SPSS and are expressed as the mean  $\pm$  SD. Each group of experiments was repeated three independent times. Differences between two groups were analyzed using one-way for intergroup analysis and independent-sample were analyzed using Tukey's test.  $P < 0.05$  indicated that the difference was statistically significant.

## Results

### MPP $\alpha$ -PDT induces apoptosis of HOS cells

To determine the toxic effect of MPP $\alpha$ -PDT on HOS cells, CCK-8 assays were performed. The results suggested that in response to PDT-24 h, MPP $\alpha$  showed a dose-dependent effect, with an IC<sub>50</sub> of 0.15  $\mu$ M (Fig. 1A), similar to the research result of Tao *et al.* [25]. Next, we added the MPP $\alpha$  (0.05, 0.10, 0.15, 0.20, 0.25, 0.30  $\mu$ M) to HOS cells after PDT treatment for 24 h, and then detected the apoptosis-related proteins cleaved-caspase 3 and cleaved PARP by western blot (Fig. 1B,C), we found that as the concentration of the photosensitizer MPP $\alpha$  increases, the expression of apoptosis-related proteins gradually increases, which was consistent with the CCK-8 results. In Hoechst staining (Fig. 1D), as indicated by the red arrow above, the apoptosis-related phenomena of nuclear pyknosis and fragmentation were clearly seen in the MPP $\alpha$ -PDT-24 h group. There were no obvious abnormalities in the Control, LED, and MPP $\alpha$  groups. Western blot and flow cytometry showed that the expression of apoptosis-related proteins (such as cleaved caspase 3 and cleaved PARP) and the rate of apoptosis in the MPP $\alpha$ -PDT-24 h group were significantly higher than those in the Control, LED and MPP $\alpha$  groups ( $P < 0.01$ ) (Fig. 1E-H). There was no obvious change in the Control, LED, and MPP $\alpha$  groups. In summary, MPP $\alpha$ -PDT can induce HOS cells to undergo apoptosis and exhibit concentration-dependent tolerance.

### MPP $\alpha$ -PDT can induce an increase in GRP78 expression

To study whether MPP $\alpha$ -PDT can induce an increase in the expression of the ER proteins, MPP $\alpha$ -PDT was used to treat HOS cells for 3, 6, 12, and 24 h to detect the GRP78, CHOP, and ATF4 expression levels. Western blot showed that MPP $\alpha$ -PDT could induce an increase in GRP78, CHOP, and ATF4 expression, and the increase was most obvious at 12 h ( $P < 0.05$ ), but there is no significant difference among the Control, LED, and MPP $\alpha$  groups (Fig. 2A,B); thus, we used MPP $\alpha$ -PDT for 12 h for the next experiment. Immunofluorescence showed that the fluorescence of GRP78 in the MPP $\alpha$ -PDT group was significantly higher than that in the Control, LED, and MPP $\alpha$  alone groups ( $P < 0.01$ ), and there was no significant change in the expression between the last three groups (Fig. 2C,D).

### Silencing of GRP78 expression reduces the proliferative activity of HOS cells

To evaluate the role of GRP78 in MPP $\alpha$ -PDT, we transfected HOS cells with siRNA-GRP78#1 and siRNA-GRP78#2 respectively, and detected the proliferation activity and GRP78 expression of the cells. We can see that both siRNA-GRP78#1 and siRNA-GRP78#2 could effectively silence the protein and mRNA expression of GRP78 in HOS cells (Fig. 3A-C). The CCK-8 assay indicated that the cell

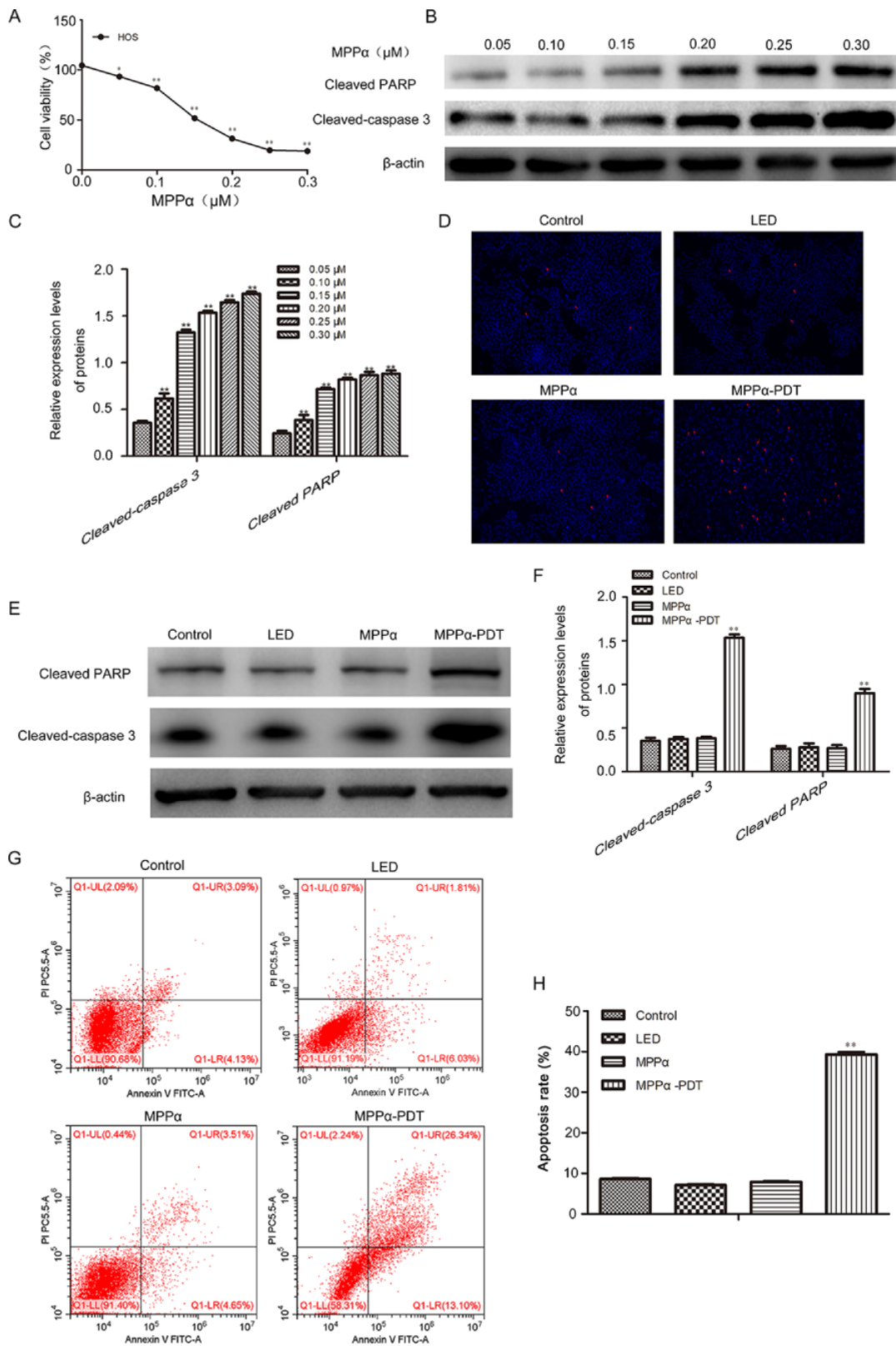


**Figure 1. MPP $\alpha$ -PDT induces apoptosis of HOS cells** (A) Cell viability was detected by CCK-8 assay at different concentrations (0.05, 0.10, 0.15, 0.20, 0.25, and 0.30  $\mu$ M) of MPP $\alpha$  with PDT treatment, and the IC<sub>50</sub> of MPP $\alpha$  was 0.15  $\mu$ M. (B,C) The different concentration of MPP $\alpha$  was added to HOS cells after PDT treatment for 24 h, the apoptosis-related proteins (cleaved-caspase 3 and cleaved PARP) were detected by western blot. (D-G) Cell apoptosis, apoptosis rate, and apoptosis-related proteins expressions were detected by Hoechst staining (magnification:  $\times$ 100), flow cytometry, and western blot, respectively. \* $P$  < 0.05, \*\* $P$  < 0.01 vs Control, LED and MPP $\alpha$  group.

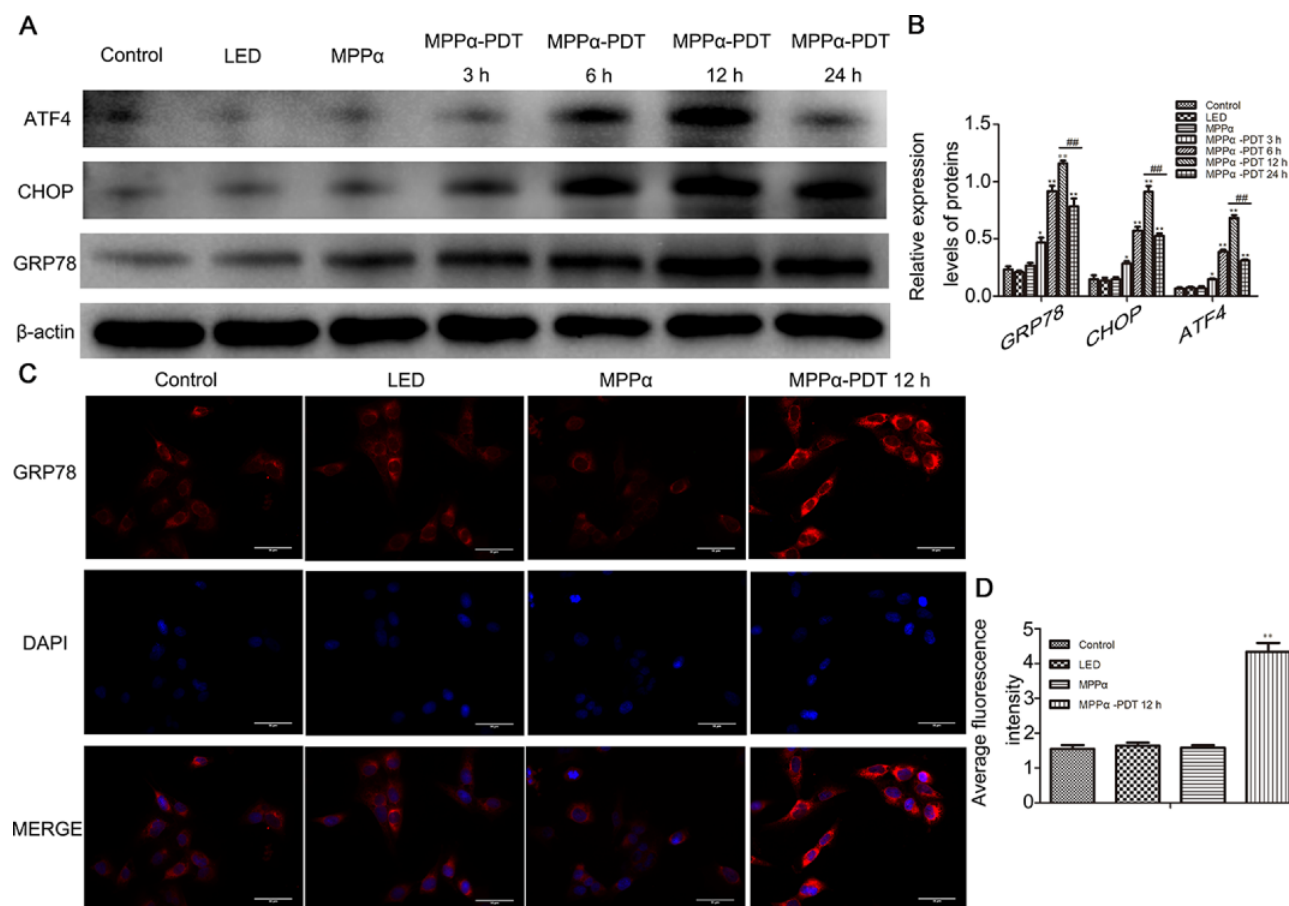


**Figure 2. MPP $\alpha$ -PDT can induce an increase of GRP78 expression** (A,B) The ER stress related proteins expression levels were detected by western blot at different time points. (C,D) The fluorescence of GRP78 was detected by immunofluorescence. \* $P < 0.05$ , \*\* $P < 0.01$  vs Control group; ## $P < 0.01$  vs MPP $\alpha$ -PDT 24 h group.

proliferation activity of the siRNA-GRP78#1 and siRNA-GRP78#2 groups were significantly lower than that of the siRNA-NC group (Fig. 3D,E). In addition, the interference effect of siRNA-GRP78#1 group was better than that of siRNA-GRP78#2 group, furthermore, siRNA-GRP78#1 inhibits the proliferation activity of HOS cells more strongly, so we chose siRNA-GRP78#1 for the next experiment. We also found that the cell viability in the siRNA-GRP78 + MPP $\alpha$ -PDT group was significantly lower than that of the MPP $\alpha$ -PDT group ( $P < 0.05$ ). Similar results were obtained for cell proliferation-related proteins (Ki67 and PCNA) (Fig. 3F,G). In summary, the effective silencing of GRP78 can reduce the proliferation activity of HOS cells and simultaneously enhance the inhibitory effect of MPP $\alpha$ -PDT on cell proliferation activity.

#### Silencing GRP78 expression increases the apoptosis level of HOS cells

To test whether silencing GRP78 can increase the sensitivity of HOS cells to MPP $\alpha$ -PDT, western blot was used to detect apoptosis-related proteins (cleaved-caspase 3, cleaved PARP) (Fig. 4A,B). The indicated proteins were expressed at significantly higher levels in the siRNA-GRP78#1 group than in the siRNA-NC group, and the proteins were expressed at significantly higher levels in the siRNA-GRP78#1 + MPP $\alpha$ -PDT group than in the MPP $\alpha$ -PDT group ( $P < 0.05$ ). In addition, flow cytometry showed that

the apoptosis rates were expressed at significantly higher levels in the siRNA-GRP78#1 group than in the siRNA-NC group, and the proteins were expressed at significantly higher levels in the siRNA-GRP78#1 + MPP $\alpha$ -PDT group than in the MPP $\alpha$ -PDT group (Fig. 4C,D). In summary, after silencing GRP78, HOS cells were sensitive to MPP $\alpha$ -PDT.

#### Silencing GRP78 expression can inhibit the MPP $\alpha$ -PDT-induced activation of the Wnt pathway in HOS cells

The Wnt/ $\beta$ -catenin signaling pathway is a classic drug resistance pathway that mainly activates the downstream *ABC2* gene to cause tumor cells to resist radiotherapy and chemotherapy, leading to tumor recurrence and metastasis.  $\beta$ -catenin, as a key signaling molecule of the Wnt signaling pathway, is regulated by the upstream molecules GSK3 $\beta$  and AKT. The phosphorylation of these molecules promotes the activation of the downstream molecule  $\beta$ -catenin, and after  $\beta$ -catenin enters the nucleus and accumulates, it acts as a transcription factor to regulate downstream target genes to exert its biological effects.

In our experiments, we observed that the expression of Wnt/ $\beta$ -catenin pathway-related proteins was increased after HOS cells were treated with MPP $\alpha$ -PDT (Fig. 5A-C) ( $P < 0.05$ ), indicating that the resistance of HOS cells to MPP $\alpha$ -PDT may be related

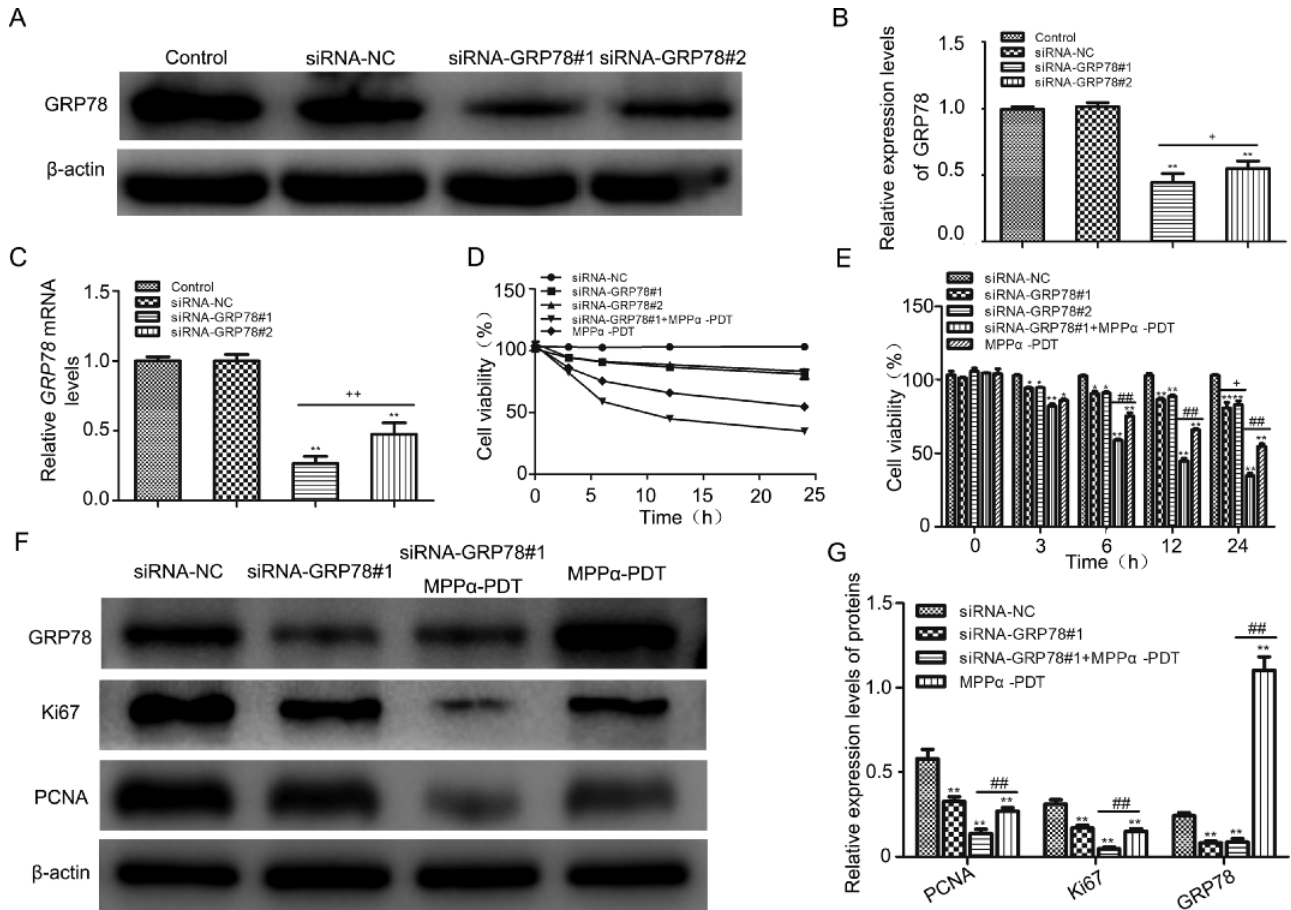


**Figure 3.** Silencing GRP78 expression reduces the proliferative activity of HOS human osteosarcoma cells (A–C) The transfection efficiency of siRNA-GRP78#1 and siRNA-GRP78#2 in HOS cells was detected by western blot and qPCR. (D,E) Cell viability was detected by CCK-8 assay at different time points after MPP $\alpha$ -PDT treatment. (F,G) Proliferation-related proteins (PCNA and Ki67) were detected by western blot. \* $P < 0.05$ , \*\* $P < 0.01$  vs Control group and siRNA-NC group; ## $P < 0.01$  vs MPP $\alpha$ -PDT group. + $P < 0.05$ , ++ $P < 0.01$  vs siRNA-GRP78#1 group.

to the activation of the Wnt/ $\beta$ -catenin pathway. Compared with those in the siRNA-NC group, the Wnt/ $\beta$ -catenin pathway-related proteins in the siRNA-GRP78#1 group were downregulated; in addition, compared with those in the MPP $\alpha$ -PDT group, the Wnt/ $\beta$ -catenin pathway-related proteins in the siRNA-GRP78#1 + MPP $\alpha$ -PDT group were significantly decreased ( $P < 0.01$ ). We also tested the content of  $\beta$ -catenin in the nucleus, and the results were similar to previous results (Fig. 5D,E). In short, siRNA-GRP78 not only downregulates the components of the Wnt/ $\beta$ -catenin signaling pathway in HOS cells but also inhibits the MPP $\alpha$ -PDT-induced activation of the Wnt/ $\beta$ -catenin pathway.

#### Silencing GRP78 can increase ROS levels in HOS cells

PDT can activate ER stress and transfer related electrons and superoxide radical anions to rapidly increase the levels of ROS in cells, thereby killing tumor cells. To test whether silencing GRP78 can increase ROS levels, we used fluorescence (Fig. 6A) and flow cytometry (Fig. 6B,C) to detect the ROS levels. We can see that compared with that in the siRNA-NC group, the average ROS fluorescence intensity in the siRNA-GRP78#1 group and the MPP $\alpha$ -PDT group increased, indicating that one of the mechanisms by which MPP $\alpha$ -PDT kills tumor cells is to increase the ROS levels. And that silencing GRP78 can also increase the ROS levels; compared with that in

the MPP $\alpha$ -PDT group, ROS levels was significantly increased in the siRNA-GRP78#1 + MPP $\alpha$ -PDT group. In summary, silencing GRP78 can increase the sensitivity of HOS cells to MPP $\alpha$ -PDT by upregulating ROS levels.

#### Discussion

PDT is a new method for treating tumors with a significant therapeutic effect. MPP $\alpha$ , as a new second-generation photosensitizer, can be specifically enriched at the tumor site, and then, the tumor can be irradiated with light of a specific wavelength to cause the photosensitizer to undergo a photochemical reaction and produce a large amount of ROS, causing tumor cell apoptosis [23,26,27]. After tumor cells are subjected to unfavorable external stimuli, they quickly undergo ER stress, activate the unfolded protein response, restore the stability of the tumor cell ER microenvironment, and enhance the adaptability of the tumor cells to external stimuli [28–30]. Our experiment showed that after MPP $\alpha$ -PDT acts on HOS cells, HOS cells undergo apoptosis and can activate the unfolded protein response to increase the expression of GRP78.

As a multifunctional protein folding partner and coreceptor, GRP78 has powerful antiapoptotic properties, plays a key role in human development and diseases and is closely related to the occurrence and development of tumors [31,32]. In tumor cells, GRP78 can

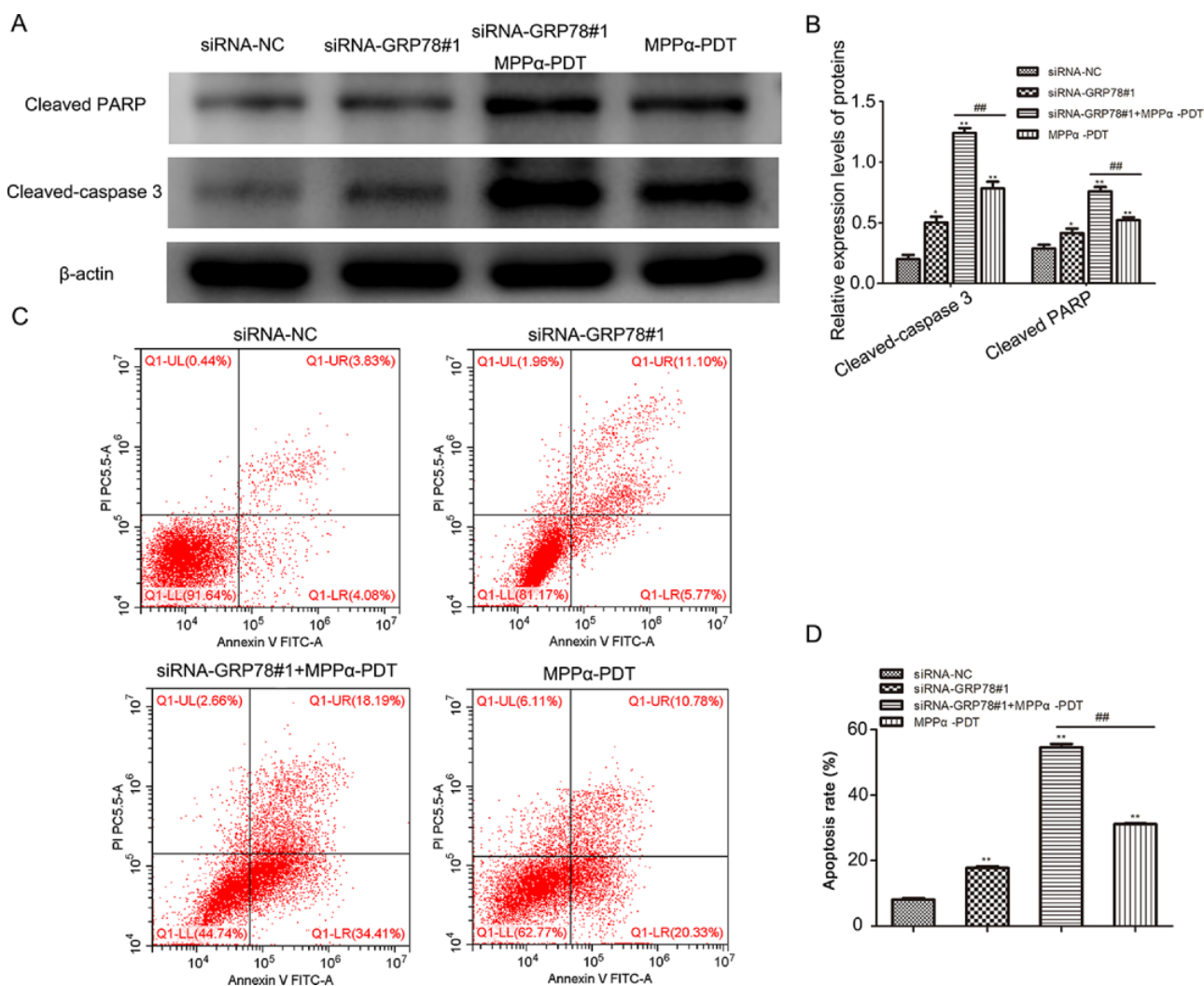


**Figure 4. Silencing GRP78 expression increases the apoptosis level of HOS cells** (A,B) Apoptosis-related proteins (cleaved-caspase 3 and cleaved PARP) were detected by western blot. (C,D) The apoptosis rates were detected by flow cytometry. \* $P < 0.05$ , \*\* $P < 0.01$  vs siRNA-NC group; ## $P < 0.01$  vs MPP $\alpha$ -PDT group.

activate the ‘pro-survival’ pathway, promote tumor cell proliferation and anti-apoptosis mechanisms, enhance the adaptability of tumor cells to adverse stimuli, and render tumor cells resistant to radiotherapy and chemotherapy, leading to tumor metastasis and recurrence [33,34]. In pancreatic ductal cell carcinoma, GRP78 expression is high in tumor tissues, and it is related to tumor resistance to chemotherapy and recurrence [35]. In glioblastoma multiforme, cells with higher GRP78 expression exhibit stronger proliferation and tumorigenicity [36]. In our study, after siRNA-GRP78 silenced the expression of GRP78 in HOS cells, the proliferation-related protein levels and proliferation activity of the HOS cells decreased, and the apoptosis-related protein levels were upregulated, indicating that GRP78 plays an anti-apoptosis and pro-proliferation role in HOS cells.

The importance of GRP78 has been confirmed in research on various cancer cells. In the present study, it is believed that GRP78 mainly promotes tumor invasion and metastasis by activating the classic Wnt/ $\beta$ -catenin signaling pathway [37,38]. In liver cancer, GRP78 activates the Wnt signaling pathway by targeting LRP6 to promote the invasion and metastasis of liver cancer [39]. In colon

cancer, silencing GRP78 can inhibit Wnt signaling *in vitro* by interfering with the glycosylation of Wnt ligands, thereby enhancing the sensitivity of colon cancer stem cells to chemotherapeutics [40]. In breast cancer, the proliferation and migration of breast cancer cells are related to the activation of the Wnt signaling pathway, and the drug isoliquiritin, which targets GRP78, enhances the sensitivity of tumor cells to chemotherapy drugs by inhibiting the Wnt signaling pathway [41,42]. In a study of osteosarcoma, it was found that chemotherapy drugs can induce the activation of the Wnt pathway in tumor cells, and inhibiting this pathway can increase the sensitivity of osteosarcoma cells to chemotherapy [43]. The Wnt/ $\beta$ -catenin signaling pathway is a classic drug resistance pathway that plays a key role in the proliferation of tumor cells.  $\beta$ -catenin, as a key signaling molecule of the Wnt signaling pathway, is regulated by the upstream molecules GSK3 $\beta$  and AKT. The phosphorylation of these molecules promotes the activation of the downstream molecule  $\beta$ -catenin, and  $\beta$ -catenin accumulates after entering the nucleus and acts as a transcription factor to regulate downstream target genes to exert its biological effect [41]. In previous experiments, we found that MPP $\alpha$ -PDT cannot completely kill HOS cells, which indicates that HOS

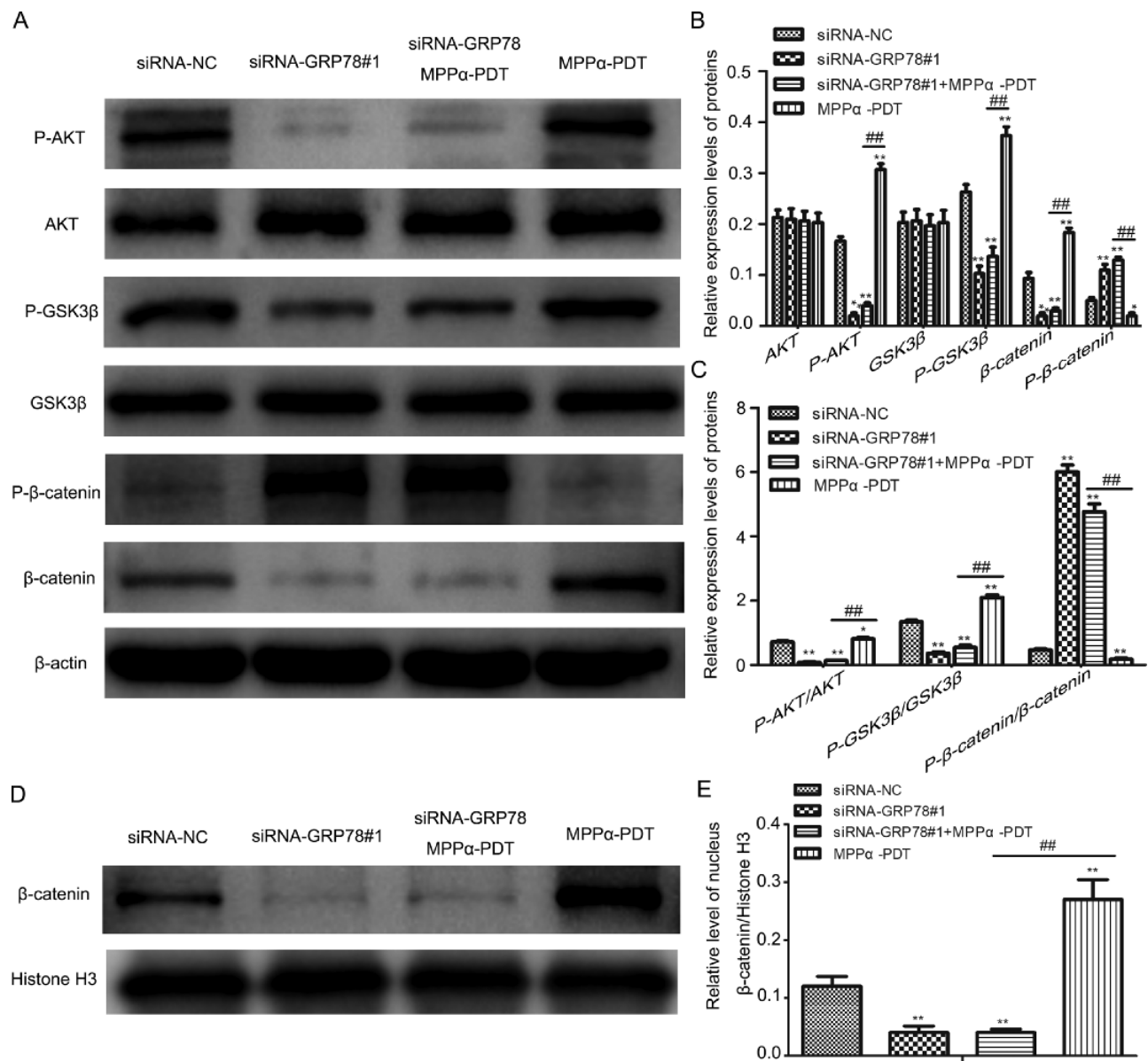


**Figure 5. Silencing GRP78 expression can inhibit the MPP $\alpha$ -PDT-induced activation of the Wnt pathway in HOS cells** (A–E) The Wnt/ $\beta$ -catenin signaling pathway-related proteins and  $\beta$ -catenin protein in the nucleus were detected by western blot. \* $P < 0.05$ , \*\* $P < 0.01$  vs siRNA-NC group; ## $P < 0.01$  vs MPP $\alpha$ -PDT group.

cells have a certain tolerance to MPP $\alpha$ -PDT [25]. Our experimental study found that the expression of Wnt pathway-related proteins increased after HOS cells were treated with MPP $\alpha$ -PDT, indicating that MPP $\alpha$ -PDT can induce the activation of the Wnt pathway in HOS cells, further showing that HOS cell tolerance to MPP $\alpha$ -PDT therapy may be related to Wnt pathway activation. In addition, after silencing GRP78, MPP $\alpha$ -PDT-induced HOS cell Wnt pathway activation was effectively inhibited, increasing the sensitivity of HOS cells to MPP $\alpha$ -PDT therapy.

ROS levels is one of the main mechanisms that kill tumor cells [44,45], and the same phenomenon has been found in PDT [46,47]. After silencing the expression of GRP78, we also detected the ROS levels. In the experiment, we found that compared with the siRNA-NC, silencing GRP78 expression increased the ROS levels; more interestingly, ROS production in the

siRNA-GRP78#1 + MPP $\alpha$ -PDT group was significantly higher than that in the MPP $\alpha$ -PDT group. The results described above indicate that silencing GRP78 enhances the sensitivity of HOS cells to MPP $\alpha$ -PDT therapy by up-regulating ROS levels.

Taken together, HOS cells were treated with MPP $\alpha$ -PDT, and the expression of GRP78 was increased. After effectively silencing GRP78 expression, the proliferation activity of HOS cells decreased and the apoptosis-related protein expression increased. In addition, silencing GRP78 expression inhibited the MPP $\alpha$ -PDT-induced activation of the Wnt pathway in HOS cells and stimulated the production of ROS levels, suggesting that silencing GRP78 increases the sensitivity of HOS cells to MPP $\alpha$ -PDT, which is related to inhibiting Wnt/ $\beta$ -catenin pathway activation and increasing ROS levels. However, the relationship between the Wnt/ $\beta$ -catenin pathway and ROS levels requires further study. So, in which silencing of the



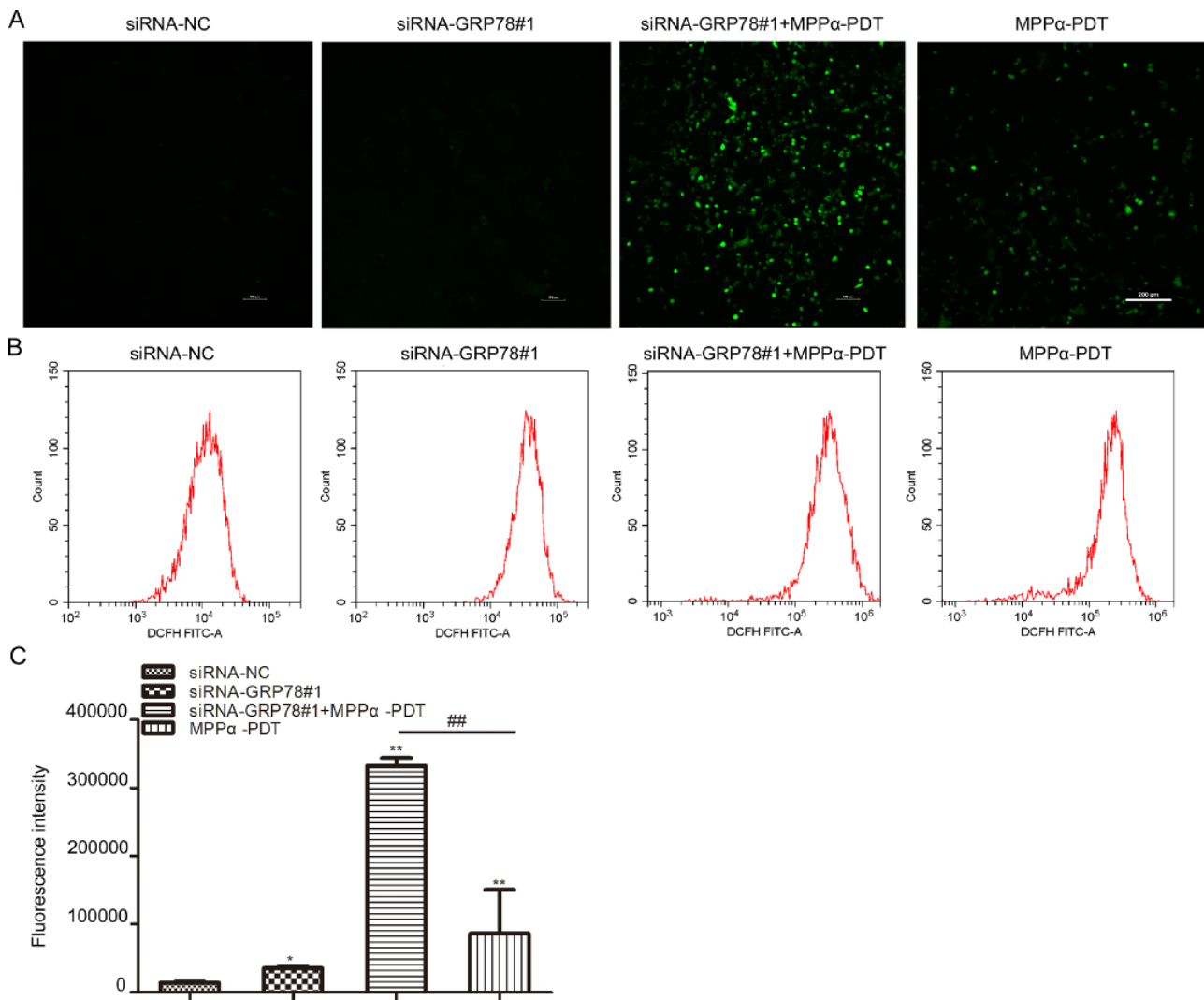


**Figure 6. Silencing GRP78 can upregulate ROS in HOS cells** The average fluorescence intensity of ROS was detected by fluorescence (magnification:  $\times 100$ ) (A) and flow cytometry (B,C) to detect the ROS levels. \* $P < 0.05$ , \*\* $P < 0.01$  vs siRNA-NC group; ## $P < 0.01$  vs MPP $\alpha$ -PDT group.

GRP78 protein was combined with MPP $\alpha$ -PDT, provides experimental evidence for the treatment of osteosarcoma. However, the lack of GRP78 overexpression experiments as a limitation of the present study and an aim of future studies.

## Funding

This work was supported by the grants from the National Natural Science Foundation of China (No. 81572634), the Natural Science Foundation of Chongqing (No. cstc2019jcyj-msxmX0358), the Basic Research and Frontiers Exploration Project of Yuzhong District, Chongqing (No. 2018114), and the Science and Technology Innovation Project for Postgraduate of Chongqing Municipal Education Commission (No. CYS18200).

## Conflict of Interest

The authors declare that they have no conflict of interest.

## References

- Wu Y, Zhou L, Wang Z, Wang X, Zhang R, Zheng L, Kang T. Systematic screening for potential therapeutic targets in osteosarcoma through a kinome-wide CRISPR-Cas9 library. *Cancer Biol Med* 2020, 17: 782–794.
- Cao D, Lei Y, Ye Z, Zhao L, Wang H, Zhang J, He F, *et al.* Blockade of IGF/IGF-1R signaling axis with soluble IGF-1R mutants suppresses the cell proliferation and tumor growth of human osteosarcoma. *Am J Cancer Res* 2020, 10: 3248–3266.
- Tu P, Huang Q, Ou Y, Du X, Li K, Tao Y, Yin H. Aloe-emodin-mediated photodynamic therapy induces autophagy and apoptosis in human osteosarcoma cell line MG63 through the ROS/JNK signaling pathway. *Oncol Rep* 2016, 35: 3209–3215.
- Li KT, Chen Q, Wang DW, Duan QQ, Tian S, He JW, Ou YS, *et al.* Mitochondrial pathway and endoplasmic reticulum stress participate in the photosensitizing effectiveness of AE-PDT in MG63 cells. *Cancer Med* 2016, 5: 3186–3193.
- Khorsandi K, Hosseinzadeh R, Chamani E. Molecular interaction and cellular studies on combination photodynamic therapy with rutoside for melanoma A375 cancer cells: an in vitro study. *Cancer Cell Int* 2020, 20: 525.
- Wang Y, Lin Y, Zhang HG, Zhu J. A photodynamic therapy combined with topical 5-aminolevulinic acid and systemic hematoporphyrin derivative is more efficient but less phototoxic for cancer. *J Cancer Res Clin Oncol* 2016, 142: 813–821.
- Cerezo M, Rocchi S. New anti-cancer molecules targeting HSPA5/BIP to induce endoplasmic reticulum stress, autophagy and apoptosis. *Autophagy* 2017, 13: 216–217.
- Gan PP, Zhou YY, Zhong MZ, Peng Y, Li L, Li JH. Endoplasmic reticulum stress promotes autophagy and apoptosis and reduces chemotherapy

- resistance in mutant p53 lung cancer cells. *Cell Physiol Biochem* 2017, 44: 133–151.
9. Niyonizigiye I, Ngabire D, Patil MP, Singh AA, Kim GD. *In vitro* induction of endoplasmic reticulum stress in human cervical adenocarcinoma HeLa cells by fucoidan. *Int J Biol Macromol* 2019, 137: 844–852.
  10. La X, Zhang L, Yang Y, Li H, Song G, Li Z. Tumor-secreted GRP78 facilitates the migration of macrophages into tumors by promoting cytoskeleton remodeling. *Cell Signal* 2019, 60: 1–16.
  11. Cultrara CN, Kozuch SD, Ramasundaram P, Heller CJ, Shah S, Beck AE, Sabatino D, et al. GRP78 modulates cell adhesion markers in prostate Cancer and multiple myeloma cell lines. *BMC Cancer* 2018, 18: 1263.
  12. Shen J, Ha DP, Zhu G, Rangel DF, Kobiela A, Gill PS, Groshen S, et al. GRP78 haploinsufficiency suppresses acinar-to-ductal metaplasia, signaling, and mutant Kras-driven pancreatic tumorigenesis in mice. *Proc Natl Acad Sci USA* 2017, 114: E4020–E4029.
  13. Daneshmand S, Quek ML, Lin E, Lee C, Cote RJ, Hawes D, Cai J, et al. Glucose-regulated protein GRP78 is up-regulated in prostate cancer and correlates with recurrence and survival. *Hum Pathol* 2007, 38: 1547–1552.
  14. Dores-Silva PR, Cauvi DM, Coto ALS, Kiraly VTR, Borges JC, De Maio A. Interaction of HSPA5 (Grp78, BIP) with negatively charged phospholipid membranes via oligomerization involving the N-terminal end domain. *Cell Stress Chaperones* 2020, 25: 979–991.
  15. Zhang N, Wei ZL, Yin J, Zhang L, Wang J, Jin ZL. MiR-106a\* inhibits oral squamous cell carcinoma progression by directly targeting MeCP2 and suppressing the Wnt/beta-Catenin signaling pathway. *Am J Transl Res* 2018, 10: 3542–3554.
  16. Srivastava NS, Srivastava RAK. Curcumin and quercetin synergistically inhibit cancer cell proliferation in multiple cancer cells and modulate Wnt/beta-catenin signaling and apoptotic pathways in A375 cells. *Phytomedicine* 2019, 52: 117–128.
  17. Liu Y, Yang Y, Wang T, Wang L, Wang X, Li T, Shi Y, et al. Long non-coding RNA CCAL promotes hepatocellular carcinoma progression by regulating AP-2alpha and Wnt/beta-catenin pathway. *Int J Biol Macromol* 2018, 109: 424–434.
  18. Huang X, Chen J, Wu W, Yang W, Zhong B, Qing X, Shao Z. Delivery of MutT homolog 1 inhibitor by functionalized graphene oxide nanoparticles for enhanced chemo-photodynamic therapy triggers cell death in osteosarcoma. *Acta Biomater* 2020, 109: 229–243.
  19. Morgan J, Whitaker JE, Oseroff AR. GRP78 induction by calcium ionophore potentiates photodynamic therapy using the mitochondrial targeting dye victoria blue BO. *Photochem Photobiol* 1998, 67: 155–164.
  20. Purushothaman B, Lee J, Hong S, Song JM. Multifunctional TPP-PEG-biotin self-assembled nanoparticle drug delivery-based combination therapeutic approach for co-targeting of GRP78 and lysosome. *J Nanobiotechnology* 2020, 18: 102.
  21. Gabrysiak M, Wachowska M, Barankiewicz J, Pilch Z, Ratajska A, Skrzypek E, Winiarska M, et al. Low dose of GRP78-targeting subtilase cytotoxin improves the efficacy of photodynamic therapy *in vivo*. *Oncol Rep* 2016, 35: 3151–3158.
  22. Firczuk M, Gabrysiak M, Barankiewicz J, Domagala A, Nowis D, Kujawa M, Jankowska-Steifer E, et al. GRP78-targeting subtilase cytotoxin sensitizes cancer cells to photodynamic therapy. *Cell Death Dis* 2013, 4: e741.
  23. Chen Y, Yin H, Tao Y, Zhong S, Yu H, Li J, Bai Z, et al. Antitumor effects and mechanisms of pyropheophorbide-alpha methyl ester-mediated photodynamic therapy on the human osteosarcoma cell line MG63. *Int J Mol Med* 2020, 45: 971–982.
  24. Livak KJ, Schmittgen TD. Analysis of relative gene expression data using real-time quantitative PCR and the 2(-Delta Delta C(T)) Method. *Methods* 2001, 25: 402–408.
  25. Tao Y, Ou Y, Yin H, Chen Y, Zhong S, Gao Y, Zhao Z, et al. Establishment and characterization of human osteosarcoma cells resistant to pyropheophorbide-alpha methyl ester-mediated photodynamic therapy. *Int J Oncol* 2017, 51: 1427–1438.
  26. Huang L, Chen Q, Yu L, Bai D. Pyropheophorbide-alpha methyl ester-mediated photodynamic therapy induces apoptosis and inhibits LPS-induced inflammation in RAW264.7 macrophages. *Photodiagnosis Photodyn Ther* 2019, 25: 148–156.
  27. Huang Q, Ou YS, Tao Y, Yin H, Tu PH. Apoptosis and autophagy induced by pyropheophorbide-alpha methyl ester-mediated photodynamic therapy in human osteosarcoma MG-63 cells. *Apoptosis* 2016, 21: 749–760.
  28. Xin D, Quan R, Zeng L, Xu C, Tang Y. Lipoxin A4 protects rat skin flaps against ischemia-reperfusion injury through inhibiting cell apoptosis and inflammatory response induced by endoplasmic reticulum stress. *Ann Transl Med* 2020, 8: 1086.
  29. Wang X, Chen B, Xu D, Li Z, Sui Y, Lin X. Delicaflavone reverses cisplatin resistance via endoplasmic reticulum stress signaling pathway in non-small cell lung cancer cells. *Oncotargets Ther* 2020, 13: 10315–10322.
  30. Shin DH, Leem DG, Shin JS, Kim JI, Kim KT, Choi SY, Lee MH, et al. Compound K induced apoptosis via endoplasmic reticulum Ca(2+) release through ryanodine receptor in human lung cancer cells. *J Ginseng Res* 2018, 42: 165–174.
  31. Clarke WR, Amundadottir L, James MA. CLPTM1L/CRR9 ectodomain interaction with GRP78 at the cell surface signals for survival and chemoresistance upon ER stress in pancreatic adenocarcinoma cells. *Int J Cancer* 2019, 144: 1367–1378.
  32. Wang C, Cai L, Liu J, Wang G, Li H, Wang X, Xu W, et al. MicroRNA-30a-5p inhibits the growth of renal cell carcinoma by modulating GRP78 expression. *Cell Physiol Biochem* 2017, 43: 2405–2419.
  33. Raiter A, Lipovetsky J, Hyman L, Mugami S, Ben-Zur T, Yerushalmi R. Chemotherapy controls metastasis through stimulatory effects on GRP78 and its transcription factor CREB3L1. *Front Oncol* 2020, 10: 1500.
  34. Gopal U, Mowery Y, Young K, Pizzo SV. Targeting cell surface GRP78 enhances pancreatic cancer radiosensitivity through YAP/TAZ protein signaling. *J Biol Chem* 2019, 294: 13939–13952.
  35. Gifford JB, Huang W, Zeleniak AE, Hindoyan A, Wu H, Donahue TR, Hill R. Expression of GRP78, master regulator of the unfolded protein response, increases chemoresistance in pancreatic ductal adenocarcinoma. *Mol Cancer Ther* 2016, 15: 1043–1052.
  36. Dadey DYA, Kapoor V, Hoyer K, Khudanyan A, Collins A, Thotala D, Hallahan DE. Antibody targeting GRP78 enhances the efficacy of radiation therapy in human glioblastoma and non-small cell lung cancer cell lines and tumor models. *Clin Cancer Res* 2017, 23: 2556–2564.
  37. Lei Z, Yang L, Yang Y, Yang J, Niu Z, Zhang X, Song Q, et al. Activation of Wnt/beta-catenin pathway causes insulin resistance and increases lipogenesis in HepG2 cells via regulation of endoplasmic reticulum stress. *Biochem Biophys Res Commun* 2020, 526: 764–771.
  38. Li Z, Wang Y, Wu H, Zhang L, Yang P, Li Z. GRP78 enhances the glutamine metabolism to support cell survival from glucose deficiency by modulating the beta-catenin signaling. *Oncotarget* 2014, 5: 5369–5380.
  39. Xiong H, Xiao H, Luo C, Chen L, Liu X, Hu Z, Zou S, et al. GRP78 activates the Wnt/HOXB9 pathway to promote invasion and metastasis of hepatocellular carcinoma by chaperoning LRP6. *Exp Cell Res* 2019, 383: 111493.
  40. van Lidth de Jeude JF, Meijer BJ, Wielenga MCB, Spaan CN, Baan B, Rosekrans SL, Meisner S, et al. Induction of endoplasmic reticulum stress by deletion of Grp78 depletes Apc mutant intestinal epithelial stem cells. *Oncogene* 2017, 36: 3397–3405.
  41. Wang N, Wang Z, Peng C, You J, Shen J, Han S, Chen J. Dietary compound isoliquiritigenin targets GRP78 to chemosensitize breast cancer stem cells via beta-catenin/ABCG2 signaling. *Carcinogenesis* 2014, 35: 2544–2554.
  42. Tang H, Peng F, Huang X, Xie X, Chen B, Shen J, Gao F, et al. Neoisoliquiritigenin inhibits tumor progression by targeting

- GRP78-beta-catenin signaling in breast cancer. *Curr Cancer Drug Targets* 2018, 18: 390–399.
43. Martins-Neves SR, Paiva-Oliveira DI, Wijers-Koster PM, Abrunhosa AJ, Fontes-Ribeiro C, Bovee JV, Cleton-Jansen AM, *et al.* Chemotherapy induces stemness in osteosarcoma cells through activation of Wnt/beta-catenin signaling. *Cancer Lett* 2016, 370: 286–295.
  44. Pandey V, Tripathi A, Rani A, Dubey PK. Deoxyelephantopin, a novel naturally occurring phytochemical impairs growth, induces G2/M arrest, ROS-mediated apoptosis and modulates lncRNA expression against uterine leiomyoma. *Biomed Pharmacother* 2020, 131: 110751.
  45. Zhu X, Liu Y, Yuan G, Guo X, Cen J, Gong Y, Liu J, *et al.* In situ fabrication of MS@MnO<sub>2</sub> hybrid as nanozymes for enhancing ROS-mediated breast cancer therapy. *Nanoscale* 2020, 12: 22317–22329.
  46. Wei C, Li X. The role of photoactivated and non-photoactivated verteporfin on tumor. *Front Pharmacol* 2020, 11: 557429.
  47. Khorsandi K, Hosseinzadeh R, Chamani E. Molecular interaction and cellular studies on combination photodynamic therapy with rutoside for melanoma A375 cancer cells: an in vitro study. *Cancer Cell Int* 2020, 20: 525.